Chapter 6
Biomechanical Modeling of the Brain for Computer-Assisted Neurosurgery

K. Miller, A. Wittek, and G. Joldes

6.1 Introduction

During neurosurgery, the brain significantly deforms. Despite the enormous complexity of the brain (see Chap. 2) many aspects of its response can be reasonably described in purely mechanical terms, such as displacements, strains and stresses. They can therefore be analyzed using established methods of continuum mechanics. In this chapter, we discuss approaches to biomechanical modeling of the brain from the perspective of two distinct applications: neurosurgical simulation and neuroimage registration in image-guided surgery. These two challenging applications are described below.[1]

6.1.1 Neurosurgical Simulation for Operation Planning, Surgeon Training and Skill Assessment

The goal of surgical simulation research is to model and simulate deformable materials for applications requiring real-time interaction. Medical applications for this include simulation-based training, skills assessment and operation planning.

Surgical simulation systems are required to provide visual and haptic feedback to a surgeon or trainee. Various haptic interfaces for medical simulation are especially

[1] Parts of this chapter were previously published in Miller et al. [1] and Wittek et al. [2].

K. Miller (✉)
Intelligent Systems for Medicine Laboratory, School of Mechanical and Chemical Engineering, The University of Western Australia, 35 Stirling Highway, Crawley/Perth, WA 6009, Australia
e-mail: kmiller@mech.uwa.edu.au

K. Miller (ed.), *Biomechanics of the Brain*, Biological and Medical Physics, Biomedical Engineering, DOI 10.1007/978-1-4419-9997-9_6,

useful for training surgeons for minimally invasive procedures (laparoscopy/interventional radiology) and remote surgery using tele-operators. These systems must compute the deformation field within a soft organ and the interaction force between a surgical tool and the tissue to present visual and haptic feedback to the surgeon. Haptic feedback must be provided at frequencies of at least 500 Hz [3]. From a solid-mechanical perspective, the problem involves large deformations, non-linear material properties and non-linear boundary conditions. Moreover, it requires extremely efficient solution algorithms to satisfy stringent requirements on the frequency of haptic feedback. Surgical simulation is a very challenging problem of solid mechanics.

When a simulator is intended to be used for surgeon training, a generic model developed from average organ geometry and material properties can be used in computations. However, when the intended application is for operation planning, the computational model must be patient-specific. This requirement adds to the difficulty of the problem – the question of how to rapidly generate patient-specific computational models still awaits a satisfactory answer.

6.1.2 Image Registration in Image-Guided Neurosurgery

One common element of most new therapeutic technologies, such as gene therapy, stimulators, focused radiation, lesion generation, nanotechnological devices, drug polymers, robotic surgery and robotic prosthetics, is that they have extremely localized areas of therapeutic effect. As a result, they have to be applied precisely in relation to the patient's current (i.e. intra-operative) anatomy, directly over the specific location of anatomic or functional abnormality [4]. Nakaji and Speltzer [5] list the "accurate localization of the target" as the first principle in modern neurosurgical approaches.

As only pre-operative anatomy of the patient is known precisely from medical images (usually magnetic resonance images – MRI), it is now recognized that the ability to predict soft organ deformation (and therefore intra-operative anatomy) during the operation is the main problem in performing reliable surgery on soft organs. In the context of brain surgery, it is very important to be able to predict the effect of procedures on the position of pathologies and critical healthy areas in the brain. If displacements within the brain can be computed during the operation, then they can be used to warp pre-operative high-quality MR images so that they represent the current, intra-operative configuration of the brain, see Fig. 6.1.

The neuroimage registration problem involves large deformations, non-linear material properties and non-linear boundary conditions as well as the difficult issue of generating patient-specific computational models. However, it is easier than the previously discussed surgical simulation problem in two important ways. Firstly, we are interested in accurate computations of the displacement field only. Accuracy of stress computations is not required. Secondly, the computations must be conducted intra-operatively, which practically means that the results should be available to an

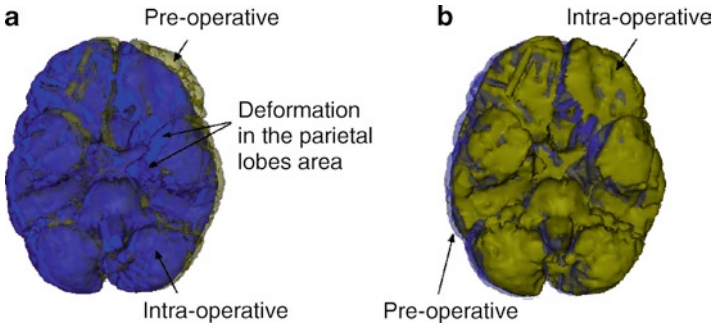

Fig. 6.1 Comparison of a brain surface determined from images acquired pre-operatively with the one determined intra-operatively from images acquired after craniotomy. Inferior (i.e. "*bottom*") view. (**a**) Pre-operative surface is semi-transparent; (**b**) Intra-operative surface is semi-transparent. Deformation of the brain surface due to craniotomy is clearly visible. Intra-operative displacements of over 20 mm have been reported in medical literature [90]. Surfaces were determined from the images provided by Department of Surgery, Brigham and Women's Hospital (Harvard Medical School, Boston, MA, USA)

operating surgeon in less than 40 s [6–9]. This still forms a stringent requirement for computational efficiency of methods used, but is much more easily satisfied than the 500 Hz haptic feedback frequency requirement for neurosurgical simulation.

Following the Introduction (Sect. 6.1), in Sect. 6.2, we describe difficulties in modeling geometry, boundary conditions, loading and material properties of the brain. In Sect. 6.3, we consider example application in the area of computational radiology. Numerical algorithms devised to efficiently solve brain deformation behavior models are described in Chap. 9. We conclude this chapter with some reflections about the state of the field.

6.2 Biomechanics of the Brain-Modelling Issues

When considering approaches to modeling the brain, one should clearly realize whether the intended application is *generic* or *patient-specific*. If the biomechanical model is constructed for a generic application, e.g. a neurosurgical simulator for surgeon training, the typical, in some sense "average", geometry and mechanical properties of an organ and tissues should be modeled. If, however, a patient-specific model is required, for example for operation planning, then clearly a "generic" model is of little utility and patient-specific data must be incorporated in the model. The reader is warned here that the question of how to generate patient-specific biomechanical models quickly and reliably remains unresolved (see Chap. 9 for current attempts to address this issue using meshless methods). Another aspect worth considering is that for computational biomechanics to be accepted and beneficial in clinical practice, biomechanical computations must be seamlessly

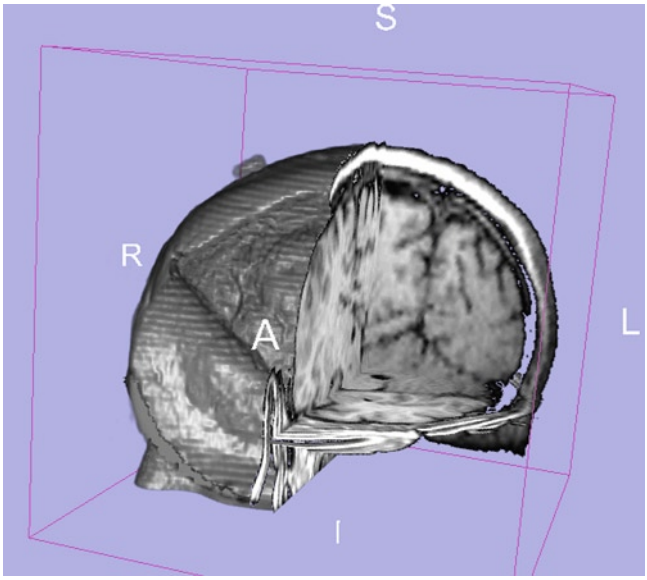

Fig. 6.2 3D magnetic resonance image (MRI) presented as a tri-planar cross-section. Slices with clearly visible tumors are shown in Sect. 6.3, Fig. 6.8. Public domain software Slicer (www.slicer.org), developed by our collaborators from Surgical Planning Laboratory, Harvard Medical School, was used to generate the image

incorporated in the clinical work flow. This can only be achieved if these computations are conducted in real or at least close to real-time (how to achieve this is discussed in Chap. 9).

In the remainder of this section, we will discuss the main modeling issues: geometry, boundary conditions, loading and tissue mechanical properties.

6.2.1 Geometry

Detailed geometric information is needed to define the domain in which the deformation field needs to be computed. Such information is provided by electronic brain atlases described in detail in Chap. 2. In applications that do not require patient-specific data (such as neurosurgical simulators for education and training), the geometric information provided by these atlases is sufficient. However, other applications such as neurosurgical simulators for operation planning and image registration systems do require patient-specific data. This patient-specific data can be obtained from radiological images (for examples see Fig. 6.2 and Chap. 3); however, the quality is significantly inferior to the data available from anatomical atlases (see Chap. 2).

The accuracy of neurosurgery is not better than 1 mm [4]. Voxel size in high-quality pre-operative MR images is usually of similar magnitude. Therefore, we can conclude

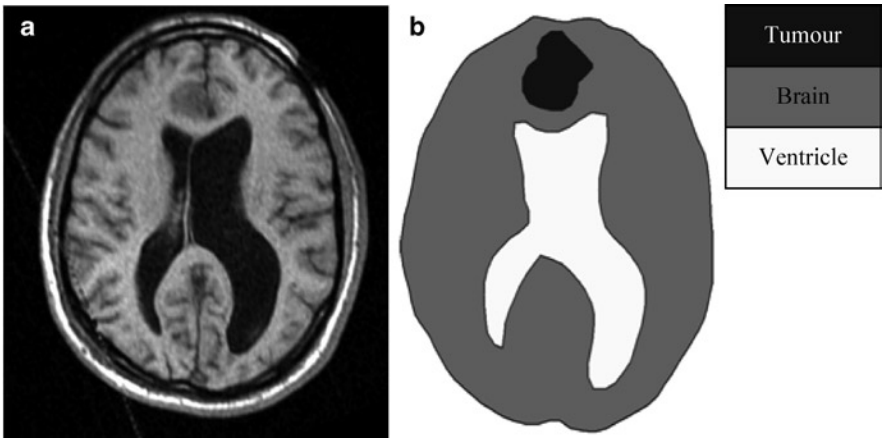

Fig. 6.3 (**a**) 2D slice of 3D brain MR volume; (**b**) Segmented image. Such "hard" segmentation is necessary for finite element mesh development

that patient-specific models of the brain geometry can be constructed with approximately 1 mm accuracy, and that higher accuracy is probably not required. The question arises, however, of which brain structures should be explicitly included in the model and which omitted? As described in Chap. 2, anatomists recognize well over a 1,000 structures within the brain. Very little (if anything) is known about relative mechanical properties of these structures. Therefore, even the most sophisticated models used by the scientific community only include brain parenchyma, ventricles, tumor (if present) and skull. A necessary step in constructing patient-specific models of brain geometry is medical image *segmentation*. Segmentation is a process that essentially explains what is what on the image, see Fig. 6.3.

Unfortunately, despite years of effort by the medical image analysis community, a generally accepted automatic brain MRI segmentation method is not yet available. In practice, very laborious semi-automatic or manual methods are employed [2, 10]. It is clear that if one attempted to include many brain structures in the patient-specific biomechanical model, then one would need to identify them in the medical image and segment them. This is a daunting task that at the time of writing does not appear to be practical.

On the other hand, when a generic application that does not require patient-specific data is considered, the 3D geometry of essentially all structures that might possibly be of interest can be imported from electronic brain atlases. For example, a hippocampus is often of interest, and its geometry and location can be clearly seen in Fig. 2.6 of Chap. 2.

To develop a numerical model of the brain biomechanics, it is necessary to create a computational grid, which in most practical cases is a finite element mesh (or a cloud of points required by a meshless method, see also Chaps. 5 and 9). Because of the stringent computation time requirements, the mesh must be constructed using low order elements that are computationally inexpensive. The linear under-integrated hexahedron is the preferred choice.

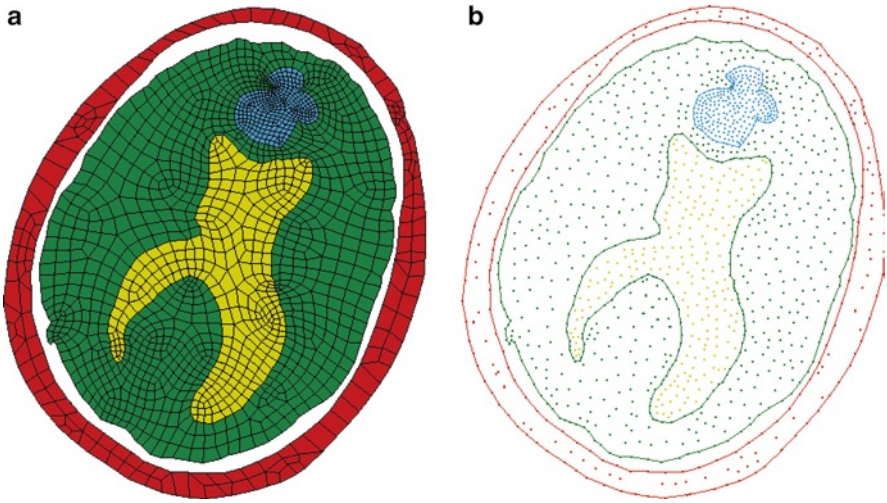

Fig. 6.4 A 2D slice of the brain discretized by (**a**) quadrilateral finite elements; and (**b**) nodes of the modified Element-Free Galerkin method. Development of a good-quality finite element mesh is time-consuming. Generation of the meshless grid is almost instantaneous

Many algorithms are now available for fast and accurate automatic mesh generation using tetrahedral elements, but not for automatic hexahedral mesh generation [11–13]. Template-based meshing algorithms can be used for discretizing different organs using hexahedrons [14–16], but these types of algorithms only work for healthy organs. In the case of severe pathologies (such as a brain tumor or severely enlarged ventricles), such algorithms cannot be used as the shape, size and position of the pathology are unpredictable. This is one reason why many authors proposed the use of tetrahedral meshes for their models [6, 8, 17, 18]. In order to automate the simulation process, mixed meshes having both hexahedral and linear tetrahedral elements are the most convenient. Examples of such meshes are shown in Fig. 6.9 in the next section.

An alternative to using the finite element method is to use one of the available meshless methods. The problem of generating the computational grid disappears as one needs only to drop a cloud of points into the volume defined by a 3D medical image [19–25], see Fig. 6.4. Details of Meshless Total Lagrangian algorithm for computing soft tissue deformations are given in Chap. 9.

6.2.2 Boundary Conditions

The formulation of appropriate boundary conditions for computation of brain deformation during surgery constitutes a significant problem because of the complexity of the brain–skull interface (see Fig. 5.3 in Chap. 5 on modeling the brain for injury prevention where this problem is also highlighted).

A number of researchers fix the brain surface to the skull [26, 27]. We do not recommend this approach. One alternative is to use a gap between the brain and the skull that allows for motion of the brain within the cranial cavity [9, 28–32]. Another alternative is to use a frictionless sliding (with separation) contact model [33, 34], which can be incorporated into finite element computations very efficiently, see Chap. 9. The reader should be warned, however, that biomechanical knowledge about the properties of the brain–skull interface is very limited [35] and the brain-skull interface models used in the literature are "best guesses" and their relation to reality is unclear.

The skull should be included in the model either explicitly or in the form of an appropriate boundary condition for the brain. As the skull is orders of magnitude stiffer than the brain tissue, its rigidity can be assumed. The spine–spinal cord interactions and constraining effects of the spinal cord on the brain's rigid body motion can be simulated by constraining the spinal end of the model.

6.2.3 Loading

We advocate loading the models through imposed displacements on the model surface, [2, 9, 30, 36] see Fig. 6.5. In the case of neurosurgical simulation, this loading will be imposed by known motion of a surgical tool. In the case of intra-operative image, registration the current (intra-operative) position of the exposed part of the brain surface can be measured using various techniques [37]. This information can then be used to define model loading.

As suggested in papers [36, 38–40] for problems where loading is prescribed as forced motion of boundaries, the unknown deformation field within the domain depends very weakly on the mechanical properties of the continuum. As this feature is of great importance in biomechanical modeling, where there are always uncertainties in patient-specific properties of tissues, it warrants more detailed discussion.

Let us look at this from the perspective of non-rigid image registration in intra-operative image-guided procedures where high-resolution pre-operative scans are warped onto lower quality intra-operative ones [7, 41]. We are particularly interested in registering high-resolution pre-operative MRIs with lower quality intra-operative imaging modalities, such as multi-planar MRIs and intra-operative ultrasound.

This problem, when viewed from the perspective of a mechanical or civil engineer, can be considered as follows: the brain, whose detailed pre-operative image is available, after craniotomy, due to a number of physical and physiological reasons, deforms (so-called brain shift). We are interested in the intra-operative (i.e. current) position of the brain, of which partial information is provided by low-resolution intra-operative images. In mathematical terms, this problem can be described by equations of solid mechanics.

Consider motion of a deforming body in a stationary co-ordinate system, Fig. 6.6.

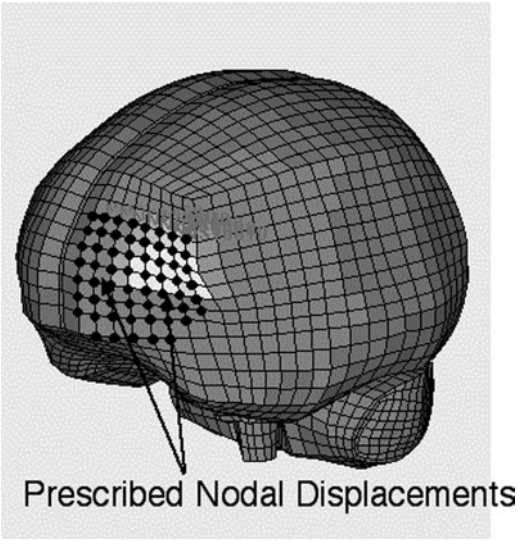

Fig. 6.5 Model loading through prescribed nodal displacements at the exposed brain surface

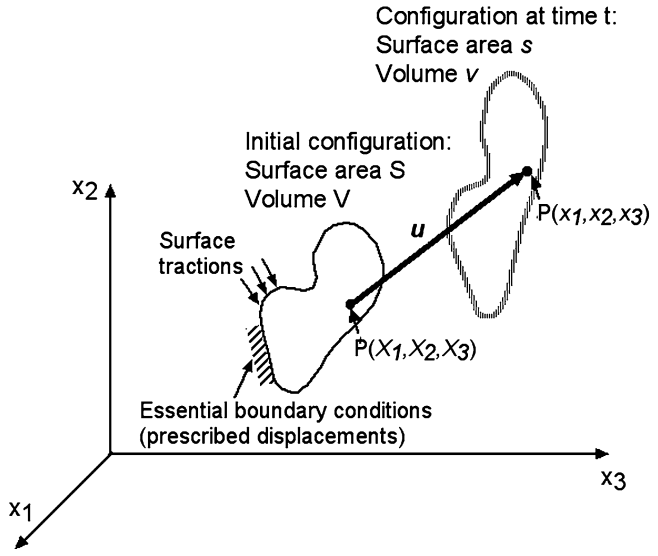

Fig. 6.6 Motion of a body in a stationary co-ordinate system. Initial configuration, described by upper case coordinates, can be considered as a high-quality pre-operative image. Current, deformed configuration (described by lower-case coordinates) is unknown; however, partial information is available from a lower resolution intra-operative image

In the analysis, we follow all particles in their motion, from the original to the final configuration of the body, which means that the Lagrangian (or material) formulation of the problem is adopted. Motion of the system sketched in Fig. 6.6 can be described by equations of motion often written in so-called weak formulation:

$$\int_v \tau_{ij}\delta\varepsilon_{ij}\,\mathrm{d}V = \int_v f_i^B \delta u_i\,\mathrm{d}V + \int_s f_i^S \delta u_i\,\mathrm{d}S, \tag{6.1}$$

where ε is the Almansi strain, $\int_v \tau_{ij}\delta\varepsilon_{ij}\,\mathrm{d}V$ is the internal virtual work, $\int_v f_i^b \delta u_{ij}\,\mathrm{d}V$ is the virtual work of external body forces (this includes inertial effects), and $\int_s f_i^s \delta u_i \mathrm{d}s$ is the virtual work of external surface forces. As the brain undergoes finite deformation, current volume V and surface S, over which the integration is to be conducted, are unknown: they are part of the solution rather than input data. Therefore, appropriate solution procedures which allow finite deformation must be used, see Chap. 9. Integral equation (9.1) must be supplemented by formulae describing the mechanical properties of materials, i.e. appropriate constitutive models. However, an important advantage of the weak formulation is that the essential (displacement) boundary conditions are automatically satisfied [42].

Boundary conditions may prescribe kinematic variables such as displacements and velocities (essential boundary conditions) or tractions (natural boundary conditions, these also include point forces). It should be noted that "boundary conditions" do not have to be applied at the physical boundary of the deforming object.

Depending on the amount of information about the intra-operative position of the brain available from intra-operative imaging modalities, brain registration can be described in mathematical terms as follows:

Case I: Entire boundary of the brain can be extracted from the intra-operative image. Mathematical description:

- Known: initial position of the domain (i.e. the brain), as determined from pre-operative MRI
- Known: current position of the entire boundary of the domain (the brain)
- Unknown: displacement field within the domain (the brain), in particular current position of the tumor and critical, from the perspective of a surgical approach, healthy tissues

No information of surface tractions is required for the solution of this problem. Problems of this type are called in theoretical elasticity "pure displacement problems" [43].

Case II: Limited information about the boundary (e.g. only the position of the brain surface exposed during craniotomy) and perhaps about current position of clearly identifiable anatomical landmarks, e.g. as described in [44]. No external forces applied to the boundary. Mathematical description:

- Known: initial position of the domain (i.e. the brain), as determined from pre-operative MRI

– Known: current position of some parts of the boundary of the domain (the brain); zero pressure and traction forces everywhere else on the boundary
– Unknown: displacement field within the domain (the brain), in particular current position of the tumor and critical healthy tissues

Problems of this type are very special cases of so-called "displacement – traction problems" that have not, to the best of our knowledge, been considered as a separate class and no special methods of solution for these problems exist. In Miller [45], it was suggested to call such problems "displacement – zero traction problems".

The solution in displacements for both pure displacement problems and displacement-zero traction problems is only very weakly sensitive to mechanical properties of the deforming continuum. To see why let us first consider an (over-simplified) linear-elastic case. Then the following simple dimensional reasoning applies: The loading is provided by the enforced motion of boundaries measured in meters [m]; the result of computations are displacements measured in [m]; therefore the result cannot depend on the stress parameter measured in [Pa = N/m^2]. We should note here that the result can depend on (dimensionless) Poisson's ratio and on (dimensionless) ratios of stress parameters if the model contains different materials with different stiffness. In the general non-linear case, the displacement results will still remain insensitive to the stress parameter appearing in the non-linear material law, but may depend on the particular form of that law. This dependency can, however, be expected to be rather weak. The explicit demonstration of this was given in [38, 40] where the shapes of compressed and extended cylinders were shown to be essentially independent of the material law used for the cylinder's material, see Fig. 6.7.

In the case of the full-scale brain deformation computation, our experience confirms the expected insensitivity of computed displacement fields to chosen tissue constitutive models [30]. This result is important because it demonstrates the utility of computational biomechanics even in the most common situation when the patient-specific mechanical properties of tissues remain unknown.

6.2.4 Models of Mechanical Properties of Brain Tissue

The first question to address is whether a single-phase continuum model for the tissue should be used or if bi-phasic and even more complicated multi-phase models are preferable. Many researchers conclude that the brain is obviously a hydrated tissue and therefore use bi-phasic models based on consolidation theory, see e.g. [46] and references cited therein. We are of the opinion that bi-phasic, consolidation theory-based models are inconsistent with brain tissue behavior observed in simple experiments. For example, no leakage of CSF was observed in brain tissue samples loaded by CSF pressure difference [47]. Another argument against using bi-phasic models is that during numerous unconfined compression experiments [48], we never

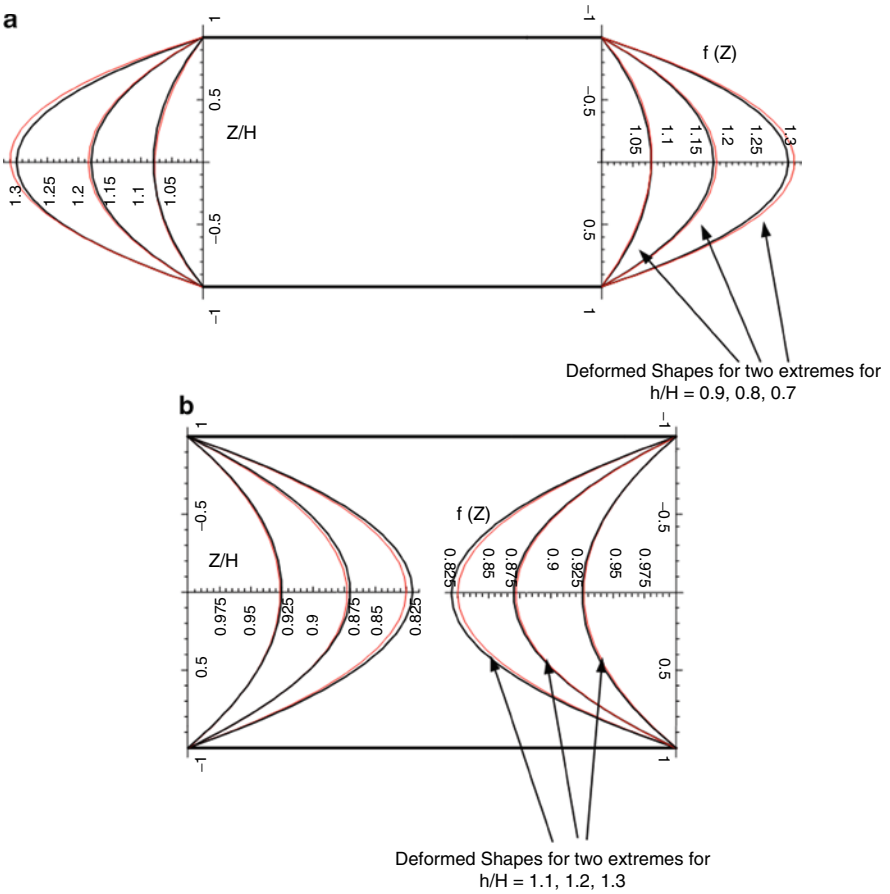

Fig. 6.7 Shapes of cylinders modeled as Extreme-Mooney and Neo-Hookean materials. (**a**) compression by 10, 20 and 30%. (**b**) extension by 10, 20 and 30%. Z/H denotes a dimensionless coordinate along the height of the cylinder. f(Z) stands for the shape of the side of the deformed cylinder. Shape of a cylinder made from a "real" material is expected to fall between the two extremes

observed fluid leaking from the side of the samples. Such leakage is predicted by a bi-phasic theory. Therefore, in the remainder of this chapter, we will discuss only single-phase modeling approaches.

Experimental results show that the mechanical response of brain tissue to external loading is very complex. The stress–strain relationship is clearly non-linear with no portion in the plots suitable for estimating a meaningful Young's modulus. It is also obvious that the stiffness of the brain in compression is much higher than in extension. The non-linear relationship between stress and strain–rate is also apparent. Detailed exposition of the current knowledge about mechanical properties of brain tissue is given in Chap. 4. Here we only discuss modeling issues directly pertinent to modeling neurosurgery.

The great majority of brain models assume brain tissue *incompressibility* and *isotropy* (see also Chaps. 4 and 5). The assumption of incompressibility is not contentious. Whether it is reasonable to assume brain tissue to be isotropic (i.e. mecha-nical properties to be the same in all directions) is less clear, especially in view of the obviously directional character of white matter fibers. Brain tissues do not normally bear mechanical loads and do not exhibit directional structure, provided that a large enough length scale is considered. Therefore, they may be assumed to be initially isotropic, see e.g. [49–57]. When modeling brain deformations during surgery, we need to keep in mind that the accuracy of displacement computations rarely needs to be better than about 1 mm – the claimed accuracy of neurosurgery. Therefore, "average isotropic" properties at the length scales relevant to surgical procedures are most probably sufficient. These properties are relatively well accounted for by an Ogden-type hyperviscoelastic model [54] described in Chap. 4, equations (4.4) and (4.5).

Average properties, such as those described above, are not sufficient for patient-specific computations of stresses and reaction forces because of the very large variability inherent to biological materials. This variability is clearly demonstrated in the biomechanics literature, see e.g. [54, 58–60]. Unfortunately, despite recent progress in elastography using ultrasound [61] and magnetic resonance [62–64], reliable methods of measuring patient-specific properties of the brain are not yet available.

Nevertheless, as shown in the previous section on modeling loading, a lot can be achieved even without a patient-specific model of brain tissue mechanical properties if the model is loaded by the enforced motion of a boundary and the problem is formulated as a pure displacement or displacement-zero traction problem. As the computed results are then almost insensitive to the assumed mechanical properties of the tissue, we advocate using the simplest model that is compatible with finite deformation solution procedures: a Neo-Hookean model:

$$ {}^{t}_{0}S = \mu J^{-2/3}\left(I_3 - \frac{1}{3} I\, {}^{t}_{0}C^{-1} \right) + k(J-1) J\, {}^{t}_{0}C^{-1}, \tag{6.2} $$

where ${}^{t}_{0}S$ is, the second Piola-Kirchhoff stress, I is the first invariant of the deviatoric Right Cauchy Green deformation tensor C (the first strain invariant), J is the determinant of the deformation gradient (representing the volume change), I_3 is the 3×3 identity matrix, μ is the shear modulus, and k is the bulk modulus of the material.

The accuracy of this approach is demonstrated in the next section.

6.2.5 Model Validation

For mathematical modeling and computer simulation to be of any practical use – to be *reliable* [65] – the results derived from the models must be known to lie within

the prescribed margins of accuracy. As we have seen in Chap. 5, ascertaining that this is the case when modeling high-speed impacts and brain injury is a very difficult task. Modelers of the brain for neurosurgery are, however, in a better position – they have to their disposal intra-operative imaging modalities (see Chap. 3) providing images that can be used for a relatively straightforward validation of the results of computer simulations of brain deformations.

Biomechanical models of the brain contain a lot of simplifying assumptions to make them mathematically and computationally tractable. To be of practical use, solutions to these models must be obtained in real or close-to-real time. Therefore, often non-standard, specially designed solution algorithms and software implementations are used (see Chap. 9). It is very important, and unfortunately overlooked by many researchers, that the biomechanical model and solution method be validated separately! For, if we evaluated a "software system" consisting of implemented non-standard solution algorithms to a complicated biomechanical model and found discrepancies when compared with experiments, we would have no indication whether these discrepancies are due to inappropriate modeling assumptions or faulty numerical procedure (or both).

We recommend that the new real-time solution algorithms be verified against well-established solution procedures implemented in commercial software. The assumptions of the biomechanical model need to be evaluated against available experimental data. The biomechanical model should then be validated by comparing the solutions computed using established numerical procedures and the experiment. If these hurdles are cleared and it can be also demonstrated that replacing established numerical procedures with the specialized ones developed for real-time applications does not affect the computed results, then one may treat the "software system" with some confidence.

How accurate should the results of the computational biomechanics model of the brain be? Accuracy of manual neurosurgery is not better than 1 mm. The voxel size of currently the best available experimental tool for model validation – the intra-operative MRI – is of the same order. Therefore, the computed intra-operative displacements do not need to be more accurate than about 1 mm. We may note here that, paradoxically, this accuracy requirement is much less stringent than what we are used to in traditional engineering disciplines. How about stresses? In image-guided surgery applications, we are not interested in stress distributions, only in the displacement field. This is one of the reasons simple constitutive models of the brain tissue can be used. However, for surgical simulation applications, we need to compute reaction forces on surgical tools that will be displayed to the user through a haptic interface. At present, there is no consensus regarding how accurate this haptic feedback should be to facilitate the user's realistic experience. Given the present state of biomechanical knowledge, the best that can be achieved is qualitative agreement between real and computed interaction forces (see e.g. [55]). This is despite examples of excellent agreement between computations and phantom experiments [66] as well as controlled in vitro experiments [67].

6.3 Application Example: Computer Simulation of the Brain Shift

A particularly exciting application of non-rigid image registration is in intra-operative image-guided procedures, where pre-operative scans are warped onto sparse intra-operative ones [7, 41]. We are especially interested in registering high-resolution pre-operative MRIs with lower quality intra-operative imaging modalities, such as multi-planar MRIs and intra-operative ultrasound. To achieve accurate matching of these modalities, precise and fast algorithms to compute tissue deformations are fundamental.

Here we present the analysis of five cases of craniotomy-induced brain shift representing different situations that may occur during neurosurgery [2].

6.3.1 Generation of Computational Grids: From Medical Images to Finite Element Meshes

Three-dimensional patient-specific brain meshes were constructed from the segmented pre-operative MRIs (Fig. 6.8) obtained from the anonymized retrospective database of Computational Radiology Laboratory (Children's Hospital, Boston, MA). The parenchyma, ventricles and tumor were distinguished in the segmentation process, Fig. 6.8.

Because of the stringent computation time requirements, the meshes had to be constructed using low order elements that are not computationally expensive. The under-integrated hexahedron with linear shape functions is the preferred choice due to its superior convergence and accuracy characteristics. To partly automate the meshing, we used mixed meshes consisting of both hexahedral and tetrahedral elements with linear shape functions (Fig. 6.9, Table 6.1). The meshes were built using IA-FEMesh (a freely available software toolkit for hexahedral mesh generation developed at the University of Iowa) [68] and HyperMesh™ (a high-performance commercial finite element mesh generator by Altair, Ltd. of Troy, MI, USA). Following the literature [69, 70], hexahedral elements with Jacobian of below 0.2 were regarded as unacceptably poor quality and replaced with the tetrahedral elements. Because of irregular geometry of ventricles and tumor, vast majority of tetrahedral elements were located in the ventricles and tumor as well as in the adjacent parenchyma areas. It took between 1 and 2 working days for a graduate student (assisted by an experienced finite element analyst) to generate the brain mesh for each of the craniotomy cases analyzed in this study.

As the parenchyma was modeled as an incompressible continuum, average nodal pressure (ANP) formulation by [71] was applied to prevent volumetric locking (i.e. artificial stiffening due to incompressibility) in the tetrahedral elements. We refer to these elements as non-locking ones.

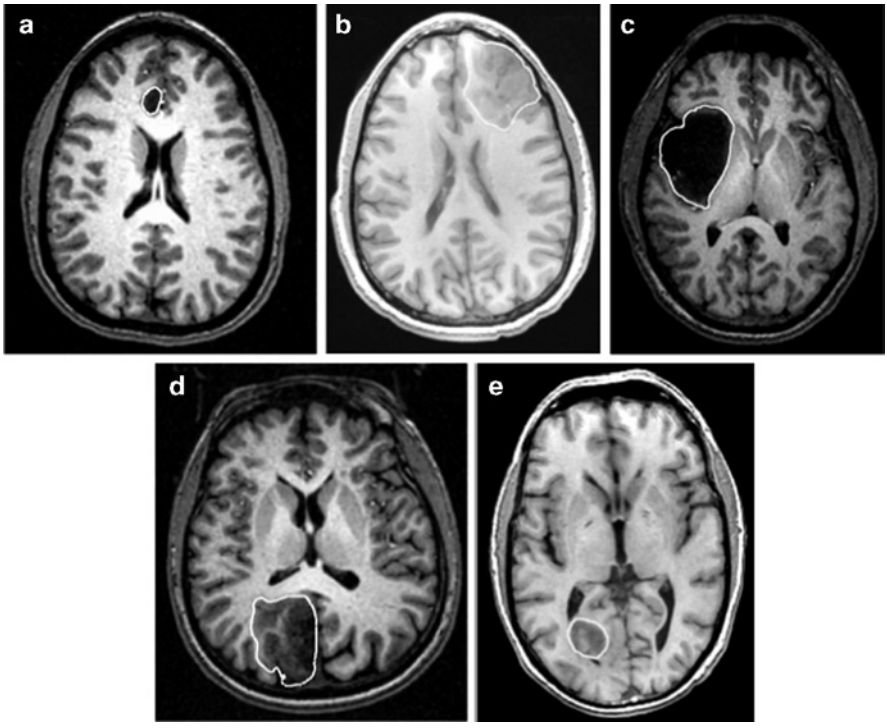

Fig. 6.8 Pre-operative T1 MRI showing tumor location in five craniotomy cases analyzed in this study. *White lines* indicate the tumor segmentations

To eliminate instabilities (known as zero-energy modes or hourglassing) that arise from single-point integration, the stiffness-based hourglass control method by [72] was used for under-integrated hexahedral elements.

The non-locking tetrahedron and the hourglass control method are described in detail in Chap. 9.

6.3.2 Loading, Boundary Conditions and Brain Tissue Constitutive Model

There are always uncertainties regarding the patient-specific properties of the living tissues. To reduce the effects of such uncertainties, we loaded the models by prescribing displacements on the exposed (due to craniotomy) part of the brain surface (Fig. 6.5). As discussed in Sect. 6.2.3, for this type of loading the unknown deformation field within the brain depends very weakly on the mechanical properties of the brain tissues. The displacements for loading the models were determined from distances between the pre-operative and intra-operative cortical

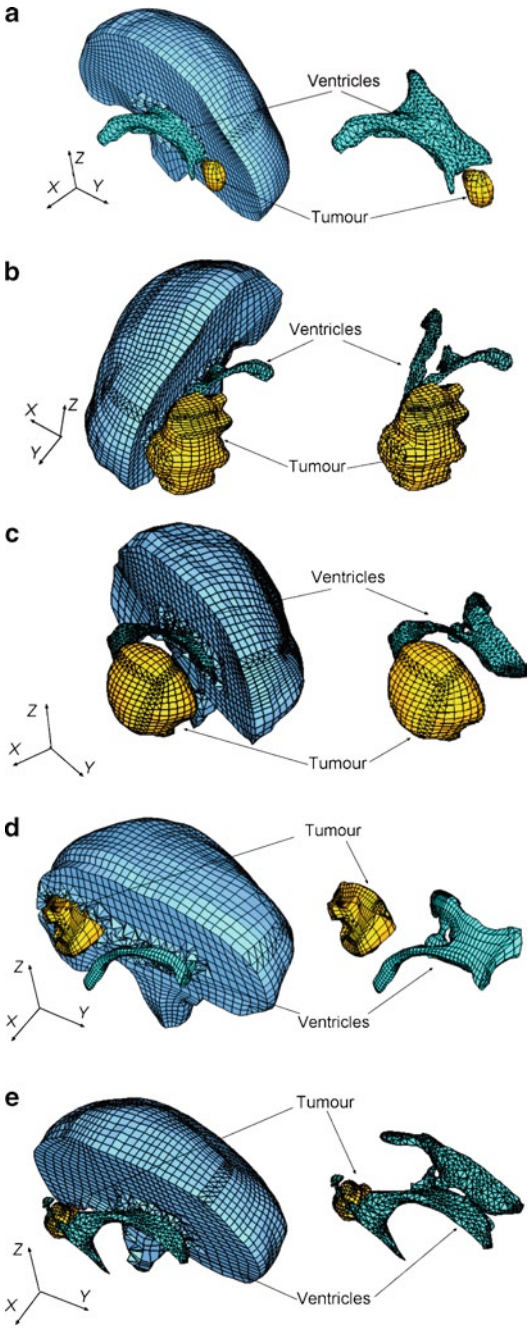

Fig. 6.9 Patient-specific brain meshes. (**a**) Case 1; (**b**) Case 2; (**c**) Case 3; (**d**) Case 4; (**e**) Case 5. Because of the complex geometry of ventricles and tumor, tetrahedral elements were mainly used for discretization of the ventricles and tumor as well as the adjacent parenchyma areas

Table 6.1 Summary of the patient-specific brain meshes used in this study. Every node in the mesh has three degrees of freedom

	Case 1	Case 2	Case 3	Case 4	Case 5
Number of hexahedral elements	14,447	10,258	10,127	9,032	8,944
Number of tetrahedral elements	13,563	20,316	23,275	23,688	21,160
Number of nodes	18,806	15,433	15,804	14,732	14,069

surfaces segmented in the MRIs. The correspondences between the pre-operative and intra-operative surfaces were determined by applying the vector-spline regularization algorithm to the surface curvature maps [73, 74].

To define the boundary conditions for the remaining nodes on the brain model surface, a contact interface was defined between the rigid skull model and areas of the brain surface where the nodal displacements were not prescribed. This formulation prevents the brain surface from penetrating the skull while allowing for frictionless sliding and separation between the brain and skull, see Chap. 9 for details. Although modeling of the brain-skull interactions through a sliding contact with separation may be viewed as an oversimplification since the anatomical structures forming the interface between the brain and skull are not directly represented, such modeling has been widely used in the literature when computing the brain deformations during brain shift [9, 29, 75].

Despite continuous efforts (see Chap. 4), commonly accepted non-invasive methods for determining patient-specific constitutive properties of the brain and other soft organs' tissues have not been developed yet. Constitutive models of the brain tissue applied for computing the brain deformation for non-rigid registration vary from simple linear-elastic model [76] to Ogden-type hyperviscoelasticity [9] and bi-phasic models relying on consolidation theory [77]. However, as explained in more detail in Sect. 6.2.3, the strength of the modeling approach used in this study is that the calculated brain deformations depend very weakly on the constitutive model and mechanical properties of the brain tissues. Therefore, following [33], we used the simplest hyperelastic model, the Neo-Hookean [78].

Based on the experimental data by Miller et al. [55] and Miller and Chinzei [54]), the Young's modulus of 3,000 Pa was assigned for the brain parenchyma tissue. For the tumor, we used the Young's modulus two times larger than for the parenchyma. This is consistent with the experimental data of [63]. As the brain and other very soft tissues are most often assumed to be incompressible, the Poisson's ratio of 0.49 was used for the parenchyma and tumor. Following [9], the ventricles were assigned the properties of a very soft compressible elastic solid with Young's modulus of 10 Pa and Poisson's ratio of 0.1 to account for possibility of leakage of the cerebrospinal fluid from the ventricles during surgery.

6.3.3 Results and Validation

In image-guided surgery, accuracy of tissue motion prediction is typically assessed by evaluating the accuracy of alignment between the registered position of the pre-operative image predicted by the non-rigid registration and the actual patient position established by an intra-operative image or navigation system. Universally accepted "gold standards" for such evaluation have not been developed yet [79]. Objective metrics for the alignment of the image can be provided by automated methods using image similarity metrics, e.g. Mutual Information [80, 81] and Normalized Cross-Correlation [82]. From the perspective of validation of biomechanical models for computing the deformation field within the brain, one of the key deficiencies of such metrics is that they quantify the alignment error in terms that do not have straightforward geometrical interpretation in terms of Euclidean distance. Therefore, validation of predictions obtained using biomechanical models has often been done using landmarks manually selected (by neuroradiology experts) in the MRIs [6, 29]. Although interpretation of the results of landmarks-based validation is very straightforward, the method provides accuracy estimation only at the landmark locations. Furthermore, determining these locations is typically very time-consuming and its accuracy relies on the experience of an expert [83].

Another option is to use the 95-percentile Hausdorff distance between sets; in our case non-rigidly registered pre-operative surfaces of the tumor and ventricles and surfaces of the tumor and ventricles obtained from the intra-operative image segmentation. We have followed this procedure in [2]. However, the resulting Hausdorff distances are highly sensitive to the segmentation accuracy. We feel that the qualitative results in the visual form of overlayed images are more reliable and convincing.

A detailed comparison between the contours of ventricles in the intra-operative images and the ones predicted by the finite element brain models is presented in Figs. 6.10 and 6.11. The comparison indicates good overall agreement between the predicted and actual intra-operative contours with the differences not exceeding the voxel size of the image ($0.86 \times 0.86 \times 2.5$ mm^3). However, some local misalignment between these contours is clearly visible. Examples of such misalignment include the third ventricle area in Case 2 (Figs. 6.9 and 6.11b) and the posterior horn of the left lateral ventricle in the area adjacent to the tumor in Case 5 (Fig. 6.11).

Five cases of craniotomy-induced brain shift analyzed here are characterized by tumors located in different parts of the brain. Comparison of the pre-operative, intra-operative and registered images indicates that detailed information about anatomical structures required for building accurate biomechanical models may be difficult to obtain for tumors that affect geometry of such structures. For instance, in Case 5, the posterior horn of the left lateral ventricle was compressed by the tumor. Consequently, a large part of the horn could not be seen in the pre-operative images (Fig. 6.11). This, in turn, limited the accuracy when simulating the posterior horn of the left lateral ventricle in the biomechanical model for predicting the brain deformations in Case 5, which led to local misregistration (Fig. 6.11).

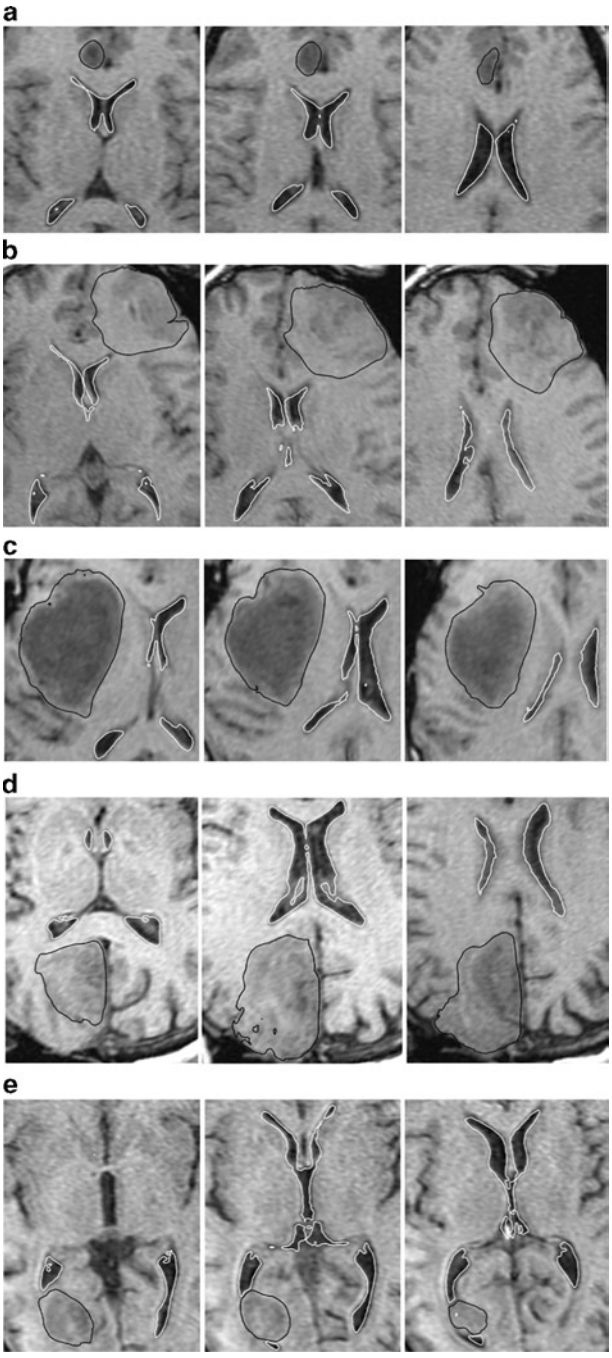

Fig. 6.10 The registered (i.e. deformed using the calculated deformation field) pre-operative contours of ventricles (*white lines*) and tumor (*black lines*) imposed on the intra-operative MRI. Three transverse image sections are presented for each case, selected so that the tumor and ventricles are clearly visible. The images were cropped and enlarged. (**a**) Case 1; (**b**) Case 2; (**c**) Case 3; (**d**) Case 4; and (**e**) Case 5. For Case 2 (*row B – left-hand-side* figure), note the differences between registered contours and intra-operative image in the third ventricle area

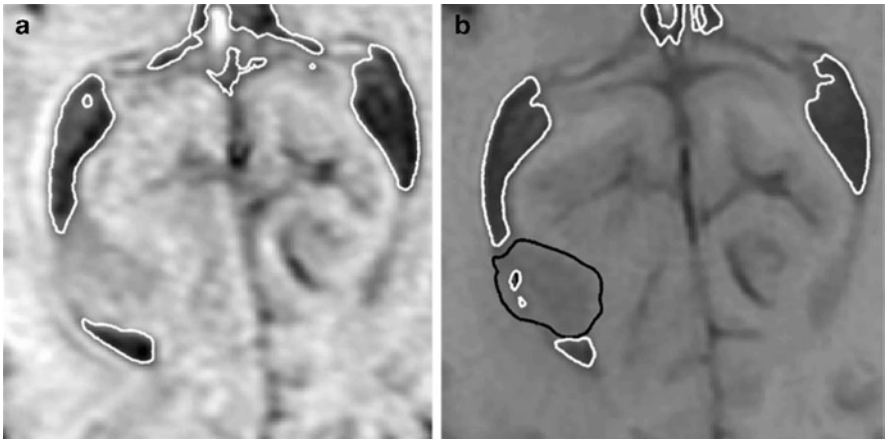

Fig. 6.11 Close-up at Case 5: (**a**) The segmented intra-operative image; (**b**) The segmented pre-operative image. Segmentation of the ventricles is indicated by *white lines* and segmentation of the tumor by *black lines*. Note the appreciable differences in shape and size of the posterior horn of left lateral ventricle between the intra-operative and pre-operative images in the area adjacent to the tumor. The horn is appreciably larger in the intra-operative than pre-operative image, which indicates that it was compressed by the tumor

6.3.4 Discussion

In this example, we used finite element meshes consisting of hexahedral and tetrahedral elements combined with the specialized non-linear (i.e. including both geometric and material non-linearities) finite element algorithms (see Chap. 9) to predict the deformation field within the brain due to craniotomy-induced brain shift. Despite abandoning unrealistic linearization (i.e. assumptions about infinitesimally small brain deformations during craniotomy and linear stress–strain relationship of the brain tissues) typically applied in biomechanical models to satisfy real-time constraints of neurosurgery, we were able to predict deformation field within the brain in less than 40 s using a standard personal computer (with a single 3 GHz dual-core processor) and less than 4 s using a graphics processing unit (NVIDIA Tesla C870) for finite element meshes of the order of 18,000 nodes and 30,000 elements (~50,000 degrees of freedom).

Despite the fact that we used only very limited intra-operative information (deformation on the brain surface exposed during the craniotomy) when prescribing loading for the models and did not have patient-specific data about the tissues' mechanical properties, our application of the specialized non-linear finite element algorithms made it possible to obtain a very good agreement between the observed positions in the intra-operative MRIs and predicted positions and deformations of the anatomical structures within the brain (Figs. 6.10 and 6.11). Nevertheless, before non-linear biomechanical models using state-of-the-art finite element algorithms, such as those applied in this example, can become a part of clinical systems for image-guided neurosurgery, reliability and accuracy of such models must be confirmed against a much larger data sample.

6.4 Conclusions

Computational mechanics has become a central enabling discipline that has led to greater understanding and advances in modern science and technology [84]. It is now in a position to make a similar impact in medicine. We have discussed modeling approaches to two applications of clinical relevance: surgical simulation and neuroimage registration. These problems can be reasonably characterized with the use of purely mechanical terms such as displacements, internal forces, etc. Therefore, they can be analyzed using the methods of continuum mechanics. Moreover, similar methods may find applications in modeling the development of structural diseases of the brain [28, 85–87].

As the brain undergoes large displacements (~10–20 mm in the case of a brain shift) and its mechanical response to external loading is strongly non-linear, we advocate the use of general, non-linear finite element procedures for the numerical solution of the proposed models.

The brain's complicated mechanical behavior – non-linear stress–strain, stress–strain rate relationships and much lower stiffness in extension than in compression – require very careful selection of the constitutive model for a given application. The selection of the constitutive model for surgical simulation problems depends on the characteristic strain rate of the process to be modeled and to a certain extent on computational efficiency considerations. Fortunately, as shown in Sect. 6.2.3 and [30], the precise knowledge of patient-specific mechanical properties of brain tissue is not required for intra-operative image registration.

A number of challenges must be met before Computer-Integrated Surgery systems based on computational biomechanical models can become as widely used as Computer-Integrated Manufacturing systems are now. As we deal with individual patients, methods to produce patient-specific computational grids quickly and reliably must be improved. Substantial progress in automatic meshing methods is required, or alternatively meshless methods may provide a solution. Computational efficiency is an important issue, as intra-operative applications, requiring reliable results within approximately 40 s, are most appealing. Progress can be made in non-linear algorithms by identifying parts that can be pre-computed, and parts that do not have to be calculated at every time step. One such possibility is to use the Total Lagrangian Formulation of the finite element method [65, 88, 89], where all field variables are related to the original (known) configuration of the system and therefore most spatial derivatives can be calculated before the simulation commences during the pre-processing stage. Implementation of algorithms in parallel on networks of processors and harnessing the computational power of graphics processing units provide a challenge for coming years.

Acknowledgements The financial support of the Australian Research Council (Grants No. DP0343112, DP0664534 and LX0560460), National Health and Medical Research Council Grant No. 1006031 and NIH (Grant No. 1-RO3-CA126466-01A1) is gratefully acknowledged. We thank our collaborators Dr Ron Kikinis and Dr Simon Warfield from Harvard Medical School and Dr Kiyoyuki Chinzei and Dr Toshikatsu Washio from Surgical Assist Technology Group of AIST, Japan, for help in various aspects of our work.

The medical images used in the present study (provided by Dr Simon Warfield) were obtained in the investigation supported by a research grant from the Whitaker Foundation and by NIH grants R21 MH67054, R01 LM007861, P41 RR13218 and P01 CA67165.

We thank Toyota Central R&D Labs. (Nagakute, Aichi, Japan) for providing the THUMS brain model.

References

1. Miller, K., Wittek, A., Joldes, G., et al.: Modelling brain deformations for computer-integrated neurosurgery. Int. J. Numer. Methods Biomed. Eng. **26**, 117–138 (2010)
2. Wittek, A., Joldes, G., Couton, M., et al.: Patient-specific non-linear finite element modelling for predicting soft organ deformation in real-time; application to non-rigid neuroimage registration. Prog. Biophys. Mol. Biol. **103**, 292–303 (2010)
3. Dimaio, S.P., Salcudean, S.E.: Interactive simulation of needle insertion models. IEEE Trans. Biomed. Eng. **52**, 1167–1179 (2005)
4. Bucholz, R., MacNeil, W., McDurmont, L.: The operating room of the future. Clin. Neurosurg. **51**, 228–237 (2004)
5. Nakaji, P., Speltzer, R.F.: The marriage of technique, technology, and judgement. Innov. Surg. Approach **51**, 177–185 (2004)
6. Ferrant, M., Nabavi, A., Macq, B., et al.: Serial registration of intraoperative MR images of the brain. Med. Image Anal. **6**, 337–359 (2002)
7. Warfield, S.K., Haker, S.J., Talos, F., et al.: Capturing intraoperative deformations: research experience at Brigham and Women's Hospital. Med. Image Anal. **9**, 145–162 (2005)
8. Warfield, S.K., Talos, F., Tei, A., et al.: Real-time registration of volumetric brain MRI by biomechanical simulation of deformation during image guided surgery. Comput. Vis. Sci. **5**, 3–11 (2002)
9. Wittek, A., Miller, K., Kikinis, R., et al.: Patient-specific model of brain deformation: application to medical image registration. J. Biomech. **40**, 919–929 (2007)
10. Joldes, G., Wittek, A., Couton, M., et al.: Real-time prediction of brain shift using nonlinear finite element algorithms. In: Medical Image Computing and Computer-Assisted Intervention – MICCAI 2009. Springer, Berlin (2009a)
11. Owen, S.J.: A survey of unstructured mesh generation technology. In: LAB, S. N., ed. 7th International Meshing Roundtable, Dearborn, Michigan, USA, pp. 239–267, October 1998
12. Owen, S.J.: Hex-dominant mesh generation using 3D constrained triangulation. Comput. Aided Des. **33**, 211–220 (2001)
13. Viceconti, M., Taddei, F.: Automatic generation of finite element meshes from computed tomography data. Crit. Rev. Biomed. Eng. **31**, 27–72 (2003)
14. Castellano-Smith, A.D., Hartkens, T., Schnabel, J., et al.: Constructing patient specific models for correcting intraoperative brain deformation. In: 4th International Conference on Medical Image Computing and Computer Assisted Intervention MICCAI, Lecture Notes in Computer Science 2208, Utrecht, The Netherlands, pp. 1091–1098 (2001)
15. Couteau, B., Payan, Y., Lavallée, S.: The Mesh-Matching algorithm: an automatic 3D Mesh generator for finite element structures. J. Biomech. **33**, 1005–1009 (2000)
16. Luboz, V., Chabanas, M., Swider, P., et al.: Orbital and maxillofacial computer aided surgery: patient-specific finite element models to predict surgical outcomes. Comput. Meth. Biomech. Biomed. Eng. **8**, 259–265 (2005)
17. Clatz, O., Delingette, H., Bardinet, E., et al.: Patient specific biomechanical model of the brain: application to Parkinson's disease procedure. In: Ayache, N., Delingette, H. (eds.) International Symposium on Surgery Simulation and Soft Tissue Modeling (IS4TM'03), pp. 321–331. Springer, Juan-les-Pins, France (2003)

18. Ferrant, M., Macq, B., Nabavi, A., et al.: Deformable modeling for characterizing biomedical shape changes. In: Borgefors, I.N.G., Sanniti di Baja, G. (eds.) Discrete Geometry for Computer Imagery: 9th International Conference, Uppsala, Sweden, pp. 235–248. Springer, London (2000)
19. Belytschko, T., Lu, Y.Y., Gu, L.: Element-free Galerkin methods. Int. J. Numer. Methods Eng. **37**, 229–256 (1994)
20. Horton, A., Wittek, A., Joldes, G., et al.: A meshless Total Lagrangian explicit dynamics algorithm for surgical simulation. Int. J. Numer. Methods Biomed. Eng. **26**, 117–138 (2010)
21. Horton, A., Wittek, A., Miller, K.: Computer simulation of brain shift using an element free galerkin method. In: Middleton, J., Jones, M. (eds.) 7th International Symposium on Computer Methods in Biomechanics and Biomedical Engineering CMBEE 2006, Antibes, France (2006a)
22. Horton, A., Wittek, A., Miller, K.: Towards meshless methods for surgical simulation. In: Computational Biomechanics for Medicine Workshop, Medical Image Computing and Computer-Assisted Intervention MICCAI 2006, Copenhagen, Denmark, pp. 34–42 (2006b)
23. Horton, A., Wittek, A., Miller, K.: Subject-specific biomechanical simulation of brain indentation using a meshless method. In: Ayache, N., Ourselin, S., Maeder, A., eds. International Conference on Medical Image Computing and Computer-Assisted Intervention MICCAI 2007, Brisbane, Australia, pp. 541–548. Springer, Berlin, 29 October to 2 November (2007)
24. Li, S., Liu, W.K.: Meshfree Particle Methods. Springer, Berlin (2004)
25. Liu, G.R.: Mesh Free Methods: Moving Beyond the Finite Element Method. CRC, Boca Raton (2003)
26. Hagemann, A., Rohr, K., Stiehl, H.S., et al.: Biomechanical modeling of the human head for physically based, nonrigid image registration. IEEE Trans. Med. Imaging **18**, 875–884 (1999)
27. Miga, M.I., Paulsen, K.D., Hoopes, P.J., et al.: In vivo quantification of a homogenous brain deformation model for updating preoperative images during surgery. IEEE Trans. Biomed. Eng. **47**, 266–273 (2000)
28. Dutta-Roy, T., Wittek, A., Miller, K.: Biomechanical modelling of normal pressure hydrocephalus. J. Biomech. **41**, 2263–2271 (2008)
29. Hu, J., Jin, X., Lee, J.B., et al.: Intraoperative brain shift prediction using a 3D inhomogeneous patient-specific finite element model. J. Neurosurg. **106**, 164–169 (2007)
30. Wittek, A., Hawkins, T., Miller, K.: On the unimportance of constitutive models in computing brain deformation for image-guided surgery. Biomech. Model. Mechanobiol. **8**, 77–84 (2009)
31. Wittek, A., Kikinis, R., Warfield, S.K., et al.: Brain shift computation using a fully nonlinear biomechanical model. In: 8th International Conference on Medical Image Computing and Computer Assisted Surgery MICCAI 2005, Palm Springs, California, USA (2005)
32. Wittek, A., Omori, K.: Parametric study of effects of brain-skull boundary conditions and brain material properties on responses of simplified finite element brain model under angular acceleration in sagittal plane. JSME Int. J. **46**, 1388–1398 (2003)
33. Joldes, G., Wittek, A., Miller, K.: Suite of finite element algorithms for accurate computation of soft tissue deformation for surgical simulation. Med. Image Anal. **13**, 912–919 (2009)
34. Joldes, G.R., Wittek, A., Miller, K., et al.: Realistic and efficient brain-skull interaction model for brain shift computation. In: Karol Miller, P.M.F.N. (ed.) Computational Biomechanics for Medicine III Workshop, MICCAI 2008, New-York, pp. 95–105 (2008)
35. Jin, X.: Biomechanical response and constitutive modeling of bovine pia-arachnoid complex. PhD thesis, Wayne State University (2009)
36. Miller, K., Wittek, A.: Neuroimage registration as displacement – zero traction problem of solid mechanics. In: Miller, K., Poulikakos, D. (eds.) Computational Biomechanics for Medicine MICCAI-associated Workshop, Copenhagen, pp. 1–14 (2006)
37. Miga, M.I., Sinha, T.K., Cash, D.M., et al.: Cortical surface registration for image-guided neurosurgery using laser-range scanning. IEEE Trans. Med. Imaging **22**, 973–985 (2003)

38. Miller, K.: How to test very soft biological tissues in extension. J. Biomech. **34**, 651–657 (2001)
39. Miller, K.: Biomechanics without mechanics: calculating soft tissue deformation without differential equations of equilibrium. In: Middleton, J., Shrive, N., Jones, M. (eds.) 5th Symposium on Computer Methods in Biomechanics and Biomedical Engineering CMBBE2004 Madrid, Spain. First Numerics (2005b)
40. Miller, K.: Method for testing very soft biological tissues in compression. J. Biomech. **38**, 153–158 (2005)
41. Ferrant, M., Nabavi, A., Macq, B., et al.: Registration of 3-D intraoperative MR images of the brain using a finite-element biomechanical model. IEEE Trans. Med. Imaging **20**, 1384–1397 (2001)
42. Fung, Y.C.: A First Course in Continuum Mechanics. Prentice-Hall, London (1969)
43. Ciarlet, P.G.: Mathematical Elasticity. North Hollad, The Netherlands (1988)
44. Nowinski, W.L.: Modified Talairach landmarks. Acta Neurochir. **143**, 1045–1057 (2001)
45. Miller, K.: Biomechanics without mechanics: calculating soft tissue deformation without differential equations of equilibrium. In: Middleton, J., Shrive, N., Jones, M. (eds.) 5th Symposium on Computer Methods in Biomechanics and Biomedical Engineering, Madrid, Spain. First Numerics (2005a)
46. Dumpuri, P., Thompson, R.C., Dawant, B.M., et al.: An atlas-based method to compensate for brain shift: preliminary results. Med. Image Anal. **11**, 128–145 (2007)
47. Dutta Roy, T.: Does normal pressure hydrocephalus have mechanistic causes? PhD Thesis, The University of Western Australia (2010)
48. Miller, K., Chinzei, K.: Constitutive modelling of brain tissue: experiment and theory. J. Biomech. **30**, 1115–1121 (1997)
49. Bilston, L., Liu, Z., Phan-Tiem, N.: Large strain behaviour of brain tissue in shear: some experimental data and differential constitutive model. Biorheology **38**, 335–345 (2001)
50. Farshad, M., Barbezat, M., Flüeler, P., et al.: Material characterization of the pig kidney in relation with the biomechanical analysis of renal trauma. J. Biomech. **32**, 417–425 (1999)
51. Mendis, K.K., Stalnaker, R.L., Advani, S.H.: A constitutive relationship for large deformation finite element modeling of brain tissue. J. Biomech. Eng. **117**, 279–285 (1995)
52. Miller, K.: Constitutive model of brain tissue suitable for finite element analysis of surgical procedures. J. Biomech. **32**, 531–537 (1999)
53. Miller, K.: Constitutive modelling of abdominal organs. J. Biomech. **33**, 367–373 (2000)
54. Miller, K., Chinzei, K.: Mechanical properties of brain tissue in tension. J. Biomech. **35**, 483–490 (2002)
55. Miller, K., Chinzei, K., Orssengo, G., et al.: Mechanical properties of brain tissue in-vivo: experiment and computer simulation. J. Biomech. **33**, 1369–1376 (2000)
56. Nasseri, S., Bilston, L.E., Phan-Thien, N.: Viscoelastic properties of pig kidney in shear, experimental results and modelling. Rheol. Acta **41**, 180–192 (2002)
57. Walsh, E.K., Schettini, A.: Calculation of brain elastic parameters in vivo. Am. J. Physiol. **247**, R637–R700 (1984)
58. Bilston, L.E., Liu, Z., Phan-Tien, N.: Linear viscoelastic properties of bovine brain tissue in shear. Biorheology **34**, 377–385 (1997)
59. Miller, K.: Biomechanics of Brain for Computer Integrated Surgery. Publishing House of Warsaw University of Technology, Warsaw (2002)
60. Prange, M.T., Margulies, S.S.: Regional, directional, and age-dependent properties of the brain undergoing large deformation. J. Biomech. Eng. **124**, 244–252 (2002)
61. Salcudean, S., Turgay, E., Rohling, R.: Identifying the mechanical properties of tissue by ultrasound strain imaging. Ultrasound Med. Biol. **32**, 221–235 (2006)
62. Mccracken, P.J., Manduca, A., Felmlee, J., et al.: Mechanical transient-based magnetic resonance elastography. Magn. Reson. Med. **53**, 628–639 (2005)
63. Sinkus, R., Tanter, M., Xydeas, T., et al.: Viscoelastic shear properties of in vivo breast lesions measured by MR elastography. Magn. Reson. Imaging **23**, 159–165 (2005)
64. Green, M.A., Bilston, L.E., Sinkus, R.: In vivo brain viscoelastic properties measured by magnetic resonance elastography. NMR Biomed. **21**(7), 755–764 (2008)

65. Bathe, K.-J.: Finite Element Procedures. Prentice-Hall, New Jersey (1996)
66. Ma, J., Wittek, A., Singh, S., et al.: Evaluation of accuracy of non-linear finite element computations for surgical simulation: study using brain phantom. Comput. Methods Biomech. Biomed. Eng. **13**, 783–794 (2010)
67. Wittek, A., Dutta-Roy, T., Taylor, Z., et al.: Subject-specific non-linear biomechanical model of needle insertion into brain. Comput. Methods Biomech. Biomed. Eng. J. **11**, 135–146 (2008)
68. Grosland, N.M., Shivanna, K.H., Magnotta, V.A., et al.: IA-FEMesh: an open-source, interactive, multiblock approach to anatomic finite element model development. Comput. Meth. Programs Biomed. **94**, 96–107 (2009)
69. Ito, Y., Shih, A.M., Soni, B.K.: Octree-based reasonable-quality hexahedral mesh generation using a new set of refinement templates. Int. J. Numer. Methods Eng. **77**, 1809–1833 (2009)
70. Shepherd, J.F., Zhang, Y., Tuttle, C.J., et al.: Quality improvement and boolean-like cutting operations in hexahedral meshes. In: 10th Conference of the International Society of Grid Generation, Crete, Greece (2007)
71. Joldes, G.R., Wittek, A., Miller, K.: Non-locking tetrahedral finite element for surgical simulation. Commun. Numer. Methods Eng. **25**, 827–836 (2008)
72. Joldes, G.R., Wittek, A., Miller, K.: An efficient hourglass control implementation for the uniform strain hexahedron using the Total Lagrangian formulation. Commun. Numer. Methods Eng. **24**, 1315–1323 (2008)
73. Arganda-Carreras, I., Sorzano, S.C.O., Marabini, R., et al.: Consistent and elastic registration of histological sections using vector-spline regularization. International Conference on Computer Vision Approaches to Medical Image Analysis. LNCS. Springer, Setubal, Portugal (2006)
74. Joldes, G.R., Wittek, A., Miller, K.: Real-time nonlinear finite element computations on GPU – application to neurosurgical simulation. Comput. Methods Appl. Mech. Eng. **199**, 3305–3314 (2010)
75. Skrinjar, O., Nabavi, A., Duncan, J.: Model-driven brain shift compensation. Med. Image Anal. **6**, 361–373 (2002)
76. Warfield, S.K., Ferrant, M., Gallez, X., et al.: Real-time biomechanical simulation of volumetric brain deformation for image guided neurosurgery. In: SC 2000: High Performance Networking and Compting Conference, Dallas, USA, pp. 1–16 (2000)
77. Miga, M.I., Roberts, D.W., Kennedy, F.E., et al.: Modeling of retraction and resection for intraoperative updating of images. Neurosurgery **49**, 75–85 (2001)
78. Yeoh, O.H.: Some forms of strain-energy function for rubber. Rubber Chem. Technol. **66**, 754–771 (1993)
79. Chakravarty, M.M., Sadikot, A.F., Germann, J., et al.: Towards a validation of atlas warping techniques. Med. Image Anal. **12**, 713–726 (2008)
80. Viola, P., Wells III, W.M.: Alignment by maximization of mutual information. Int. J. Comput. Vision **24**, 137–154 (1997)
81. Wells Iii, W.M., Viola, P., Atsumi, H., et al.: Multi-modal volume registration by maximization of mutual information. Med. Image Anal. **1**, 35–51 (1996)
82. Rexilius, J., Warfield, S., Guttmann, C., et al.: A novel nonrigid registration algorithm and applications. Medical Image Computing and Computer-Assisted Intervention – MICCAI 2001, Toronto, Cananda (2001)
83. Miga, M.I., Paulsen, K.D., Lemery, J.M., et al.: Model-updated image guidance: initial clinical experiences with gravity-induced brain deformation. IEEE Trans. Med. Imaging **18**, 866–874 (1999)
84. Oden, J.T., Belytschko, T., Babuska, I., et al.: Research directions in computational mechanics. Comput. Meth. Appl. Mech. Eng. **192**, 913–922 (2003)
85. Berger, J., Horton, A., Joldes, G., et al.: Coupling finite element and mesh-free methods for modelling brain defromations in response to tumour growth. In: Miller, K., Nielsen, P.M.F. (eds.) Computational Biomechanics for Medicine III MICCAI-Associated Workshop, 2008. MICCAI, New York (2008)

86. Miller, K., Taylor, Z., Nowinski, W.L.: Towards computing brain deformations for diagnosis, prognosis and nerosurgical simulation. J. Mech. Med. Biol. **5**, 105–121 (2005)
87. Taylor, Z., Miller, K.: Reassessment of brain elasticity for analysis of biomechanisms of hydrocephalus. J. Biomech. **37**, 1263–1269 (2004)
88. Miller, K., Joldes, G., Lance, D., et al.: Total Lagrangian explicit dynamics finite element algorithm for computing soft tissue deformation. Commun. Numer. Methods Eng. **23**, 121–134 (2007)
89. Zienkiewicz, O.C., Taylor, R.L.: The Finite Element Method. McGraw-Hill, London (2000)
90. Roberts, D.W., Hartov, A., Kennedy, F.E., et al.: Intraoperative brain shift and deformation: a quantitative analysis of cortical displacement in 28 cases. Neurosurgery **43**, 749–758 (1998)